

Effect of Size of Inhomogeneity on the Surface Wave Attenuation in Cementitious Media

D. G. Aggelis¹ and T. Shiotani²

1

Abstract: The present study focuses on surface wave propagation in cementitious material with inhomogeneity. Thin, flakey inclusions were added in contents of up to 10% by volume and different sizes inside the matrix to realistically simulate cracking. The results are focused on the attenuation created by the inhomogeneity. As damage is added up in content, the level of attenuation strongly increases for the whole examined frequency band. However, the size and the population of the inclusions present equally a strong influence on the attenuation. The distortion of the frequency content is also evaluated by spectral density functions, showing that simple waveform analysis can enhance the characterization of damage in addition to the valuable assessment based on wave velocity. DOI: [10.1061/\(ASCE\)MT.1943-5533.0000487](https://doi.org/10.1061/(ASCE)MT.1943-5533.0000487). © 2012 American Society of Civil Engineers.

CE Database subject headings: Rayleigh waves; Frequency; Damage; Ultrasonic methods; Cement; Wave attenuation.

Author keywords: Rayleigh waves; Frequency; Damage; Coherence; Ultrasound.

Introduction

Concrete structures are exposed to deterioration factors like weathering, corrosive agents, thermal expansion, and contraction or even freezing and thawing. Furthermore, they support operation loads, the own weight of the structure, and possibly dynamic overloading, like the one created by earthquakes. Most of the above factors affect primarily the surface of the structures, which is directly exposed to the atmospheric conditions and sustain maximum flexural loads. Deterioration is, therefore, bound to start from the surface in most cases. This deterioration may be manifested in the form of large cracks breaking on the surface, and microcracking propagating on the surface layer of the material. Inspection techniques based on the propagation of elastic waves have long been used for the estimation of the quality, and general condition of the material (Kaplan 1959, Popovics et al. 1990, Boyd and Ferraro 2005). The most common measurement used is the “pulse velocity”. Considering that the material is homogeneous, pulse velocity is directly related to the modulus of elasticity and correlated with the strength of the material through empirical relations. Pulse velocity is measured by the first disturbance detected from the waveform. This measurement is heavily dependent on the strength of the signal relatively to the noise level, which could be induced due to environmental conditions and equipment components. If the initial arrival of the wave is weaker than or similar to the noise level, pulse velocity is underestimated. This could certainly be the case in actual structures, where long propagation distances through damaged materials are applied. Rayleigh waves can also be excited in a concrete surface; they propagate within a penetration depth of approximately

one wave length and carry more of the excitation energy (Gudra and Stawinski 2000, Qixian and Bungey 1996). Their velocity is also related to elasticity and Poisson’s ratio (Sansalone and Carino 2004). The measurement of Rayleigh velocity is usually conducted by a reference peak point, therefore it is not directly influenced by the noise level. However, for cases of severe damage or long propagation, the strong reference cycle used for the measurement is severely distorted and makes the selection of reference points troublesome (Aggelis and Shiotani 2007). Frequency domain techniques like phase difference calculation between signals recorded at specific distances may provide solution for velocity measurement revealing also the dependence of velocity on frequency [Sachse and Pao 1978, Aggelis and Shiotani 2008a].

In addition to the wave velocity, attenuation has also been widely used for detection of microstructural changes or existence of damage (Landis and Shah 1995, Kim et al. 1991). It is calculated by the reduction of the wave amplitude between two measurement points. Attenuation has been shown more sensitive to damage or void content than wave velocity, as has been revealed in several studies (Shah et al. 2000, Aggelis and Shiotani 2007). It has also been correlated to the size of the aggregates, as well as air void size and content in hardened and fresh cementitious materials (Punurai et al. 2006, Philippidis and Aggelis 2005). Energy related parameters show strong correlation to the curing and strength of hydrating concrete (Voigt et al. 2003) as well. The sensitivity of attenuation to the microstructure is such, that the content of “heterogeneity” is not the only dominating factor; the typical size and shape of the inclusions play an equivalently important role and therefore, Rayleigh wave attenuation has been related to parameters like aggregate size, and damage content (Jacobs and Owino 2000, Owino and Jacobs 1999, Aggelis and Shiotani 2007). This sensitivity to the microstructure may complicate the assessment, but, on the other hand offers possibilities for more accurate characterization. Accurate characterization would require determination of several damage parameters like the number (or equivalent damage content) of the cracks, their typical size, as well as their orientation. Though this is a nearly impossible task, especially in situ, advanced features that are sensitive to the above damage parameters should be continuously sought for.

¹Dept. of Materials Science and Engineering, Univ. of Ioannina, 45110 Ioannina, Greece (corresponding author). E-mail: daggelis@cc.uoi.gr

²Graduate School of Engineering, Kyoto Univ., Nishikyoku, Kyoto 615-8540, Japan.

Note. This manuscript was submitted on June 13, 2011; approved on January 24, 2012; published online on January 26, 2012. Discussion period open until January 1, 2013; separate discussions must be submitted for individual papers. This paper is part of the *Journal of Materials in Civil Engineering*, Vol. 24, No. 8, August 1, 2012. ©ASCE, ISSN 0899-1561/2012/8-0-0/\$25.00.

The valuable but rough characterization based on pulse velocity can be improved by the addition of features from frequency domain, like the coherence function as will be discussed below. This feature evaluates the similarity between the received and the introduced pulse and can be applied in and outside of laboratory, because they are based on the recording of the waveform, which is standard in most contemporary relevant pieces of ultrasonic equipment. The connection between laboratory studies and in situ measurements is not always straight-forward. However, in several cases features examined in small scale studies have been successfully employed in characterization in real structures, like in the cases of (Aggelis and Shiotani 2007 and Aggelis et al. 2009b), where the frequency dependence of velocity improved the accuracy in repair efficiency evaluation.

In the present paper, elastic waves were applied on the surface of mortar specimens with inhomogeneity. In order to simulate damage, small flakey inclusions were added in different contents and sizes, and attenuation of the surface wave was calculated. The effect of both content and size of the inclusions on wave parameters is discussed by showing that the typical size of inhomogeneity is equally important to the content. In similar studies, sphere was a first approximation for the damage shape, which produces quite reliable results (Chaix et al. 2006). However, the random orientation and general shape of the actual cracks, which are simulated by thin, flakey, small inclusions in this study, complicate the anticipated results and increase experimental variance. As opposed to bulk waves, there are no widely used models that would enable the reliable prediction of wave velocity and attenuation curves. This study aims to supply more experimental data in the area of surface waves in media with randomly oriented inhomogeneity, which has not been studied as widely as stratified media (Sansalone and Carino 2004, Kim et al. 2006) and media with surface breaking cracks (Van Wijk et al. 2004, Hevin et al. 1998, Shin et al. 2010, Aggelis et al. 2009a). The results of the present study are based on a more realistic shape of small inclusions than spheres. The size and population of inclusions leave their fingerprint on the attenuation curves since large population of small inclusions impose stronger attenuation than small population of larger size. Furthermore, the application of other features from frequency domain is discussed for their contribution in damage characterization.

Experimental Process

2 The test specimens were made of cement mortar with water to cement ratio of 0.5 and sand to cement 2 by mass. The maximum sand grain size was 3 mm. Two minutes after the ingredients were mixed in a concrete mixer, vinyl inclusions were added and the mixing continued for two additional minutes. Then the mixture was cast in cubic metal forms of 150 mm side. The specimens were demolded one day later and cured in tap water for 28 days. The vinyl inclusions were added in different volume contents (specifically 1%, 5%, and 10%), while one plain mortar specimen was also cast (Aggelis and Shiotani 2008b). Vinyl inclusions were cut in small square coupons from sheets with thickness of 0.2 mm and 0.5 mm. The exact sizes of the vinyl coupons were $15 \times 15 \times 0.5$ mm, $15 \times 15 \times 0.2$ mm, $30 \times 30 \times 0.5$ mm, and $30 \times 30 \times 0.2$ mm. The small thickness of the inclusions better simulates cracks than other spherical particles. One specimen was cast for each inclusion size and content, reaching thus a total number of 13 specimens. The authors selected to apply one specimen for each class in order to simulate many different contents and sizes of damage (totally 13 cases) instead of simulating only indicatively two or three with a larger number of specimens each. This way the results of a class

can be related and compared to the neighboring classes. Also, in order to minimize local variations in inclusion content, 20 measurements were taken on the surface and the results were averaged. Specifically, the array of receivers and excitation was translated and shifted in order to include different areas of the surface and information from different possible configuration of subsurface defects. After fracturing one preliminary specimen, it was seen that the layout of the inclusions did not show any preference in orientation or tendency of conglomeration. Though the actual cracking in concrete cannot be considered absolutely randomly oriented, especially when tensile loading occurs, cracking is bound to exist in any orientation due to the irregular shape of the aggregates.

The selection of inclusions over real cracks was made in order to firmly control their content. On the other hand, the content of actual cracks cannot be controlled or measured accurately. In that case correlation with the sustained load (that is responsible for the cracks) would be available instead of the content. The authors selected to follow the known and firmly controlled content approach since in a real structure the damage may originate not only from load, but also from other degradation factors like freezing-thawing, corrosion, or alkali silica reaction.

For the ultrasonic measurements, two broadband piezoelectric transducers, Fujicermics 1045S, were placed on the specimens' surface with a distance of 40 mm, see Fig. 1. Each excitation was introduced by pencil lead break. When the pencil lead breaks, the release of stress in the surface of the concrete generates acoustic waves whose spectral content is in the range between 0 and 300 kHz. The signals were preamplified by 40 dB and digitized with a sampling rate of 10 MHz in a Mistras system of Physical Acoustics Corporation (PAC). Silicone grease was used as couplant between the sensors and the specimen.

Waveform Distortion

Fig. 2(a) shows typical waveforms captured by the two sensors mounted on the plain mortar specimen. In both of them the strong Rayleigh cycle is observed, preceded by the weaker longitudinal mode. Measuring the delay between the strong negative peaks (marked by arrows), the Rayleigh velocity is calculated at 2,116 m/s. When simulated damage is included in a content of 1%, the Rayleigh cycle is slightly distorted, as shown in Fig. 2(b). The Rayleigh velocity in this case is measured equal to 2,062 m/s. The pulse velocity, dictated by the first disturbance detected from the waveforms is essentially comparable for both cases, measured at around 4,140 m/s. This suggests that Rayleigh waves are more sensitive to the slight amount of simulated damage. When the content of damage is 10% [see Fig. 2(c)] the Rayleigh cycle is severely distorted and a reference point cannot be easily selected for the measurement. In the case the minimum point of the cycle is chosen (again marked by an arrow), the Rayleigh velocity drops to 1,770 m/s, being reduced by 17% compared to the sound material,

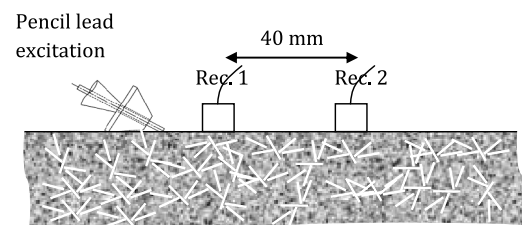


Fig. 1. Schematic representation of experimental setup

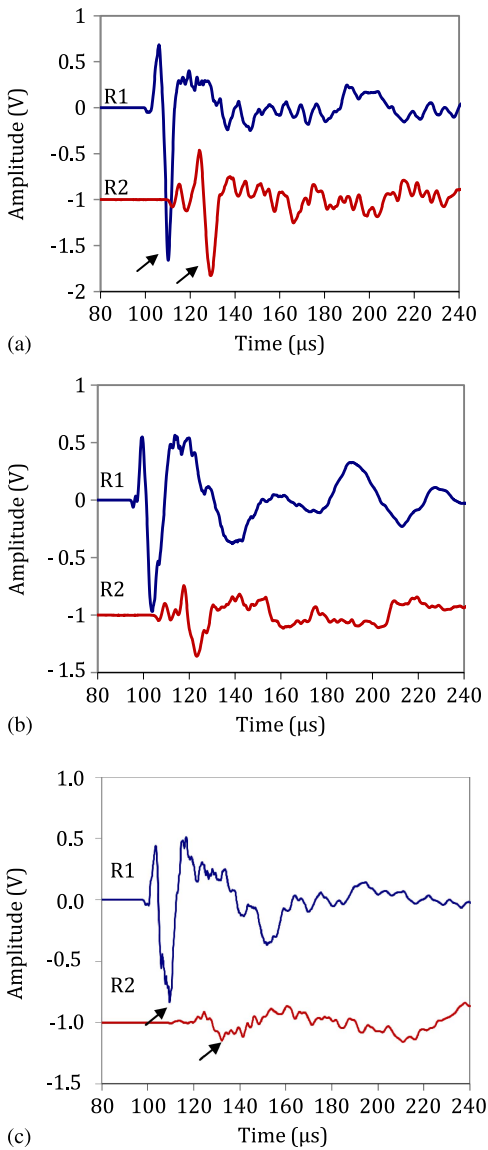


Fig. 2. Typical waveforms of first and last receiver for material with inclusions at contents 0% (a), 1% (b), and 10% (c) and inclusion size $30 \times 30 \times 0.5$ mm

while pulse velocity is measured at 3,773 m/s, with a corresponding decrease of 8.5%.

Concerning possible reflections, it is mentioned that the measurements were conducted away from the edges of the specimen. When the excitation is introduced at 50 mm from the edge, the wave from the reflection should propagate approximately 100 mm (50 mm to the edge and backward) to reach the sensors. Considering a typical velocity of 4,000 m/s for longitudinal waves, this would require 25 μ s. However, as seen from Fig. 2, the meaningful part of the signal is received well before 20 μ s. Therefore any contribution from reflection of longitudinal waves cannot strongly affect, especially taking into account the high damping characteristics of the material, which effectively diminish the energy of the wave traveling all the way to the edge and back. Concerning the Rayleigh mode that concentrates most of the energy from the excitation, their lower velocity (typically 2,000 m/s) would not allow any reflection before approximately 45 μ s, which would not at all interfere with the meaningful signal.

Spectral Distortion

Apart from the drop in the Rayleigh velocity, for high content of inclusions the signal is strongly distorted, as it is shown in Fig. 2(c). This distortion can be evaluated in the frequency domain by the coherence function (Bendat and Piersol 1993). The frequency dependent coherence $\gamma_{xy}(f)$ between two time domain waveforms $x(t)$ and $y(t)$ is a measure of the similarity of their spectral content and can be described as the corresponding of cross-correlation in the frequency domain. It is given by

$$\gamma_{xy}^2(f) = \frac{|G_{xy}(f)|^2}{G_{xx}(f)G_{yy}(f)}, \quad 0 \leq \gamma_{xy}^2(f) \leq 1 \quad (1)$$

where $G_{xy}(f)$ is the cross-spectral density function between time domain waveforms $x(t)$ and $y(t)$, while G_{xx} and G_{yy} are the auto-spectral density functions of $x(t)$ and $y(t)$.

Fig. 3 shows the coherence between signals acquired by the two sensors for different contents of inhomogeneity. The nature of the curves exhibit severe fluctuations that apart from the inhomogeneity of the material depend also on the calculation parameters chosen. In the present case coherence was calculated by embedded Matlab function with time domain window of 620 points, zero-padded to the length of 4096 points for FFT, and overlap of 528 points. It is certain that changing some parameters of the coherence calculation, this also changes the final value of the function. The reason for coherence application was the comparison of the different materials waveforms. Since all parameters are maintained constant, any differences between individual curves are attributed to the different distortion imposed by the different layout of the inclusions. In order to more clearly evaluate the difference between the coherence curves from different materials, the functions are fitted by a straight line to show their average level for comparison. It can be noted that the addition of inhomogeneity decreases the average level of spectral similarity for the band up to 400 kHz. In particular, the average coherence value drops from 0.85 for sound material to 0.68 for 10% of damage, being reduced by 20%. It is seen therefore, that the spectral similarity as evaluated by the coherence function proves very sensitive to damage. In literature it has also been used for characterization of concrete composition through ultrasonic signals (Philippidis and Aggelis 2003) and classification of acoustic emission signals (Grosse et al. 1997). In all cases the coherence function exhibits strong fluctuations throughout the examined band. However, the average value is a very reliable indicator of similarity of two signals and results in successful characterization in each case. Although straight fitting curve functions are included in Fig. 3 as indicative for the whole range, they are not necessarily the best possible fits.

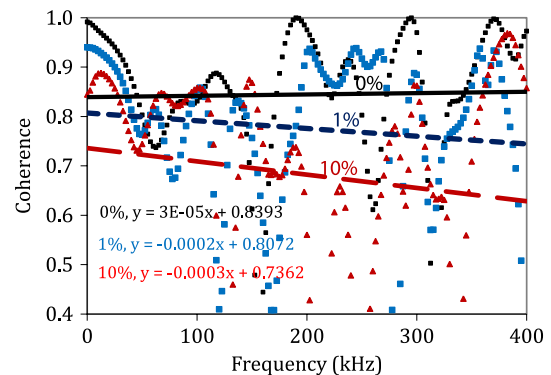


Fig. 3. Coherence function between waveforms obtained in mortar with different content of inclusions

Attenuation Curves

The comparison of the peak amplitude of waveforms captured at different positions is a measure of attenuation. Additionally, if the time domain signals are Fourier transformed their response may lead to the frequency dependent attenuation coefficient through Eq. (2):

$$a(f) = -\frac{20}{x} \log[A(f)/B(f)] \quad (2)$$

where $a(f)$ is the attenuation coefficient with respect to frequency, $A(f)$ and $B(f)$ are the FFTs of the responses of the two sensors and x is the distance between the sensors (in this case 40 mm).

Eq. (2) reveals the attenuative characteristics for specific frequency bands since the size of inhomogeneity affects individual wavelengths in a different way. This improves damage characterization capacity, especially in controlled laboratory conditions.

Effect of Inclusions' Content

Attenuation curves were calculated according to Eq. (2) for different inclusion contents. Fig. 4 shows attenuation versus frequency curves for material with inclusion size of $30 \times 30 \times 0.5$ mm. The attenuation curves of Fig. 4 are the average of 20 curves obtained at different positions on the surface of the material, as mentioned in the experimental part. The curves exhibit strong fluctuations throughout the frequency band of 0 to 400 kHz. Again the curves are indicatively fitted by straight lines. By using the trend lines, it is highlighted that a specific targeted frequency would not be reliable. As an example, for the frequency of 50 kHz, (which is close to the resonant frequency of commercial equipment), the attenuation of 1% damage is very similar to the one of 5% damage, as seen in Fig. 4. However, applying broadband equipment and taking the whole frequency range into account the two classes of material are separated by 0.0025 dB/mm.

It is seen that plain mortar exhibits the lowest attenuation, while the attenuation curve of the 10% inclusions is the highest. Even using this logarithmic unit of dB, the inclusions force an attenuation increase of approximately 200%–300% compared to the attenuation of the plain material, while at the same time they were responsible only for a slight decrease of 17% in Rayleigh velocity, as mentioned earlier. Additionally, the curve of 1% damage content is distinctly higher than plain material, showing the strong sensitivity of attenuation even to slight damage content for the band 0 – 300 kHz.

At this point it is essential to discuss on the experimental scatter, or the standard deviation of the curves, since they result from a

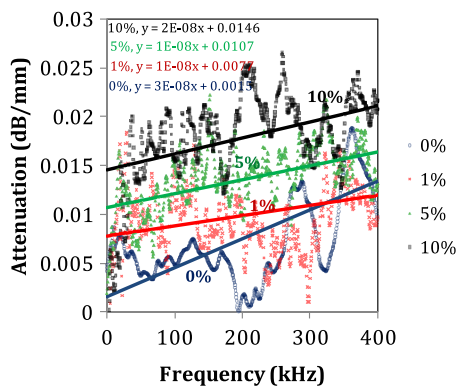


Fig. 4. Attenuation versus frequency for mortar with different inclusion contents and inclusion size $30 \times 30 \times 0.5$ mm

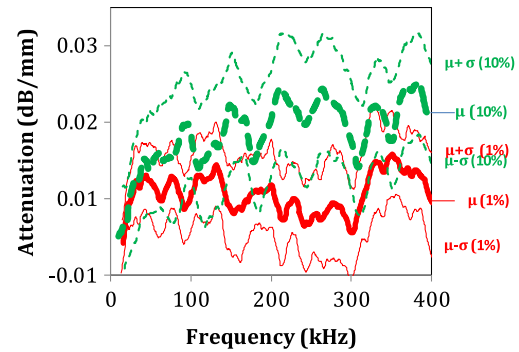


Fig. 5. Attenuation versus frequency for mortar with inclusion contents of 1% and 10% along with corresponding standard deviation

population of 20 individual curves on the surface of the specimens. These distinct curves may exhibit strong differences even though the waveforms are recorded from the surface of the same specimen. Fig. 5 indicatively shows the attenuation curves for 1% and 10% along with their standard deviation. The thick lines stand for the average curves, while the thin curves correspond to the average, μ , minus and plus standard deviation, σ , for the two types of material. The standard deviation is large, leading to strong overlaps between the different classes of materials. However, overlap is bound to exist due to the inhomogeneous nature of the materials, having local variations in the content of inclusions, as well as in the content of sand grains and air bubbles. It is mentioned that the standard deviation, σ , of the curves, averaged throughout the whole band of interest is 0.00554 dB/mm for 1% and climbs at 0.00715 dB/mm for 10% “damage”. This shows that apart from attenuation (or any other wave parameter), the experimental scatter of the measurements should also be used as an indication of damage, since the random layout of damage generally increases variability.

Effect of Inclusions' Shape

The size of the inhomogeneity plays also an important role in the wave behavior and especially in the attenuation. This is plotted in Fig. 6(a)–6(c) where the attenuation curves for different sizes of inclusions are shown for the contents of 1%, 5%, and 10% respectively. For the content of 1%, the size of $30 \times 30 \times 0.2$ mm exhibits the highest attenuation, as seen by the corresponding fitted curves in Fig. 6(a). These differences are more obvious in absolute values as the content increases. For 10% “damage”, the size of $30 \times 30 \times 0.2$ mm exhibits attenuation even more than 100% than the corresponding of $30 \times 30 \times 0.5$ mm, see Fig. 6(c). Fig. 6(c) also contains the attenuation curve of plain mortar for comparison. The measured attenuation is a result of the combined effect of geometric spreading, damping, and scattering. Geometric spreading has exactly the same effect on all curves, due to the same size of the specimens. Damping depends on the viscosity parameters of the constituents and therefore, for material with the same amount of inclusions should not lead to strong changes. The strong discrepancies between the curves within each subgraph of Fig. 6, should be attributed directly to scattering on the flakey inclusions. The different size of them imposes different scattering conditions and crucially affects the resulted wave field. This is readily seen by the vertical shift between the different attenuation curves. Despite the fluctuations, it can be mentioned that for all contents, $30 \times 30 \times 0.5$ mm exhibits the lowest attenuation curve, while the $30 \times 30 \times 0.2$ mm the highest (approximately six times higher than plain

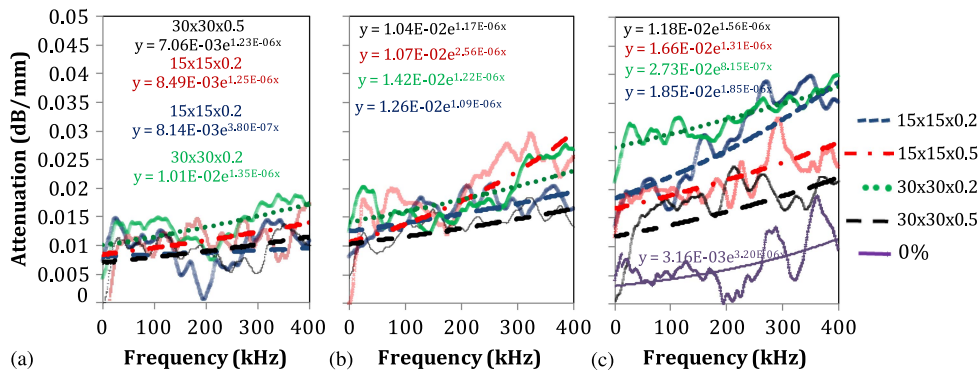


Fig. 6. Attenuation versus frequency for mortar with different inclusion size and content (a) 1%; (b) 5%; (c) 10%

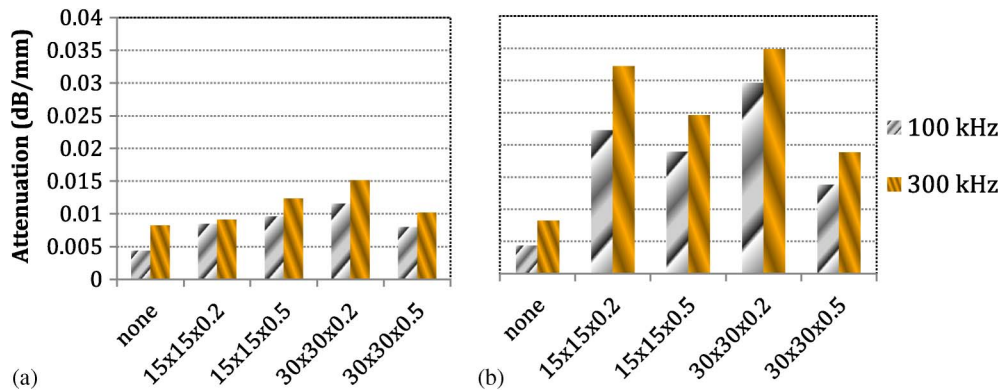


Fig. 7. Attenuation for different inclusion size and content (a) 1%; (b) 10%

material). This is reasonable because of the shape of the latter, since the volume of each inclusion is smaller, and a higher number of individual inclusions are necessary to reach the specified content. This leads to more scattering incidences as the wave propagates from the excitation point to the receivers, reducing the amplitude of the wave recorded. This finds partial confirmation in Fig. 6(c) where the inclusions of size $15 \times 15 \times 0.2$ exhibit higher attenuation than the $15 \times 15 \times 0.5$ ones.

The recorded waveforms include all different wave modes. However, it is reasonable to assume that most of the energy belongs to Rayleigh, considering that most of the energy of a point source excitation forms Rayleigh waves (Graff 1975). With Rayleigh velocities of approximately 2,000 m/s, the frequency of 100 kHz results in wavelength of 20 mm, while for 300 kHz, the wavelength is approximately 7 mm. In case of spherical inclusions, more specific conclusions concerning the size (diameter) relatively to the propagating wavelength could be drawn. For the specific case, it can be generally mentioned that two of three dimensions of the inclusions are comparable or longer to the dominant wavelengths. Apart from the direct scattering interaction of the specific shape of each inclusion with the propagating wave, the shape seems to exercise an indirect influence controlling the number of inclusions encountered by the wave front (a few large as opposed to many small). The effect of inclusion size is summarized in Fig. 7 for two indicative frequencies (100 and 300 kHz). For any content, the size $30 \times 30 \times 0.2$ mm holds the first place in attenuation almost for the whole examined band, showing that this size imposes the strongest attenuation of the Rayleigh wave, while in a similar

previous study the same size of inclusions resulted in the lowest propagation velocity as well (Aggelis and Shiotani 2008a).

Conclusions

Attenuation of Rayleigh elastic waves on cementitious material is studied in this paper. Thin, light inclusions were added in different contents and sizes to simulate distributed cracking. Parameters measured nondestructively after applying pencil lead break excitations and recording the transient responses of the surface, show sensitivity to the existence, the content, as well as the size and population of simulated cracks. These parameters originate from the time domain (wave velocity) and frequency domain (coherence and attenuation function). The results of this study are summarized below:

- The velocity of Rayleigh waves is more sensitive to inhomogeneity than of longitudinal waves (decrease of 17% and 8% respectively).
- The spectral content of the pulse is progressively distorted while propagating through mortar. This distortion is stronger for high percentage of inhomogeneity, reaching a decrease of 20% compared to the sound material.
- The attenuation of Rayleigh waves is more sensitive to damage than pulse velocity, being increased by about six times for damaged material compared to plain material.
- The size and shape of inhomogeneity exercises strong influence on attenuation. A large number of small inclusions are more effective scatterers of Rayleigh waves resulting in attenuation even double that the one of a small number of large inclusions.

It is concluded that combined information obtained by processing the waveforms may increase the descriptors in the armory of nondestructive testing toward accurate material characterization.

References

- 4 Aggelis, D. G., and Shiotani, T. (2007). "Experimental study of surface wave propagation in strongly heterogeneous media." *J. Acoust. Soc. Am.*, 122(5), EL EL151.
- 5 Aggelis, D. G., and Shiotani, T. (2008a). "Surface wave dispersion in cement-based media: inclusion size effect." *NDT & E Int.*, 41(5), 319–325.
- Aggelis, D. G., and Shiotani, T. (2008b). "Effect of inhomogeneity parameters on the wave propagation in cementitious materials." *American Concrete Institute Materials Journal*, 105(2), 187–193. (<http://www.concrete.org/PUBS/JOURNALS/OLJDetails.asp?Home=MJ&ID=19763>)
- Aggelis, D. G., Shiotani, T., and Polyzos, D. (2009a). "Characterization of surface crack depth and repair evaluation using Rayleigh waves." *Cem. Concr. Compos.*, 31(1), 77–83.
- Aggelis, D. G., Momoki, S., and Chai, H. (2009b). "Surface wave dispersion in large concrete structures." *NDT & E Int.*, 42(4), 304–307.
- Bendat, J. S., and Piersol, A. G. (1993). *Engineering Applications of Correlation and Spectral Analysis*, 2nd Ed., Wiley, New York.
- Boyd, A. J., and Ferraro, C. C. (2005). "Effect of curing and deterioration on stress wave velocities in concrete." *J. Mat. in Civ. Engrg.*, 17, 153–158.
- Chaix, J. F., Garnier, V., and Corneloup, G. (2006). "Ultrasonic wave propagation in heterogeneous solid media: Theoretical analysis and experimental validation." *Ultrasonics*, 44, 200–210.
- Graff, K. F. (1975). *Wave motion in elastic solids*, Dover Publications, New York.
- Grosse, C. U., Reinhardt, H. W., and Dahm, T. (1997). "Localization and classification of fracture types in concrete with quantitative acoustic emission measurement techniques." *NDT E Int.*, 30(4), 223–230.
- Gudra, T., and Stawinski, B. (2000). "Non-destructive characterization of concrete using surface waves." *NDT & E Int.*, 33(1), 1–6.
- Hevin, G., Abraham, O., Pedersen, H. A., and Campillo, M. (1998). "Characterisation of surface cracks with Rayleigh waves: a numerical model." *NDT and E Int.*, 31(4), 289–297.
- Jacobs, L. J., and Owino, J. O. (2000). "Effect of aggregate size on attenuation of Rayleigh surface waves in cement-based materials." *J. Eng. Mech.*, 126(11), 1124–1130.
- Kaplan, M. F. (1959). "The effects of age and water/cement ratio on the

- relation between ultrasonic pulse velocity and compressive strength." *Mag. Concr. Res.*, 11(32), 85–92.
- Kim, D. S., Seo, W. S., and Lee, K. M. (2006). "IE-SASW method for nondestructive evaluation of concrete structure." *NDT & E Int.*, 39(2), 143–154.
- Kim, Y. H., Lee, S., and Kim, H. C. (1991). "Attenuation and dispersion of elastic waves in multi-phase materials." *J. Phys. D*, 24, 1722–1728.
- Landis, E. N., and Shah, S. P. (1995). "Frequency-dependent stress wave attenuation in cement-based materials." *J. Eng. Mech.*, 121(6), 737–743.
- Owino, J. O., and Jacobs, L. J. (1999). "Attenuation measurements in cement-based materials using laser ultrasonics." *J. Eng. Mech.*, 125(6), 637–647.
- Philippidis, T. P., and Aggelis, D. G. (2003). "An acousto-ultrasonic approach for the determination of water-to-cement ratio in concrete." *Cem. Concr. Res.*, 33(4), 525–538.
- Philippidis, T. P., and Aggelis, D. G. (2005). "Experimental study of wave dispersion and attenuation in concrete." *Ultrasonics*, 43(7), 584–595.
- Popovics, S., Rose, J. L., and Popovics, J. S. (1990). "The behavior of ultrasonic pulses in concrete." *Cem. Concr. Res.*, 20, 259–270.
- Punurai, W., Jarzynski, J., Qu, J., Kurtis, K. E., and Jacobs, L. J. (2006). "Characterization of entrained air voids in cement paste with scattered ultrasound." *NDT & E Int.*, 39(6), 514–524.
- Qixian, L., and Bungey, J. H. (1996). "Using compression wave ultrasonic transducers to measure the velocity of surface waves and hence determine dynamic modulus of elasticity for concrete." *Constr Build Mater*, 10(4), 237–242.
- Sachse, W., and Pao, Y. H. (1978). "On the determination of phase and group velocities of dispersive waves in solids." *J. Appl. Phys.*, 49(8), 4320–4327.
- Sansalone, M., and Carino, N. J. (2004). "Stress wave propagation methods." in *CRC Handbook on Nondestructive Testing of Concrete*, V. M. Malhotra, and N. J. Carino, eds., CRC Press, Boca Raton FL, 275–304.
- Shah, S. P., Popovics, J. S., Subramanian, K. V., and Aldea, C. M. (2000). "New directions in concrete health monitoring technology." *J. Eng. Mech.*, 126(7), 754–760.
- Shin, S. W., Min, J., and Lee, J. Y. (2010). "Effect of concrete compositions in energy transmission of surface waves for nondestructive crack depth evaluation." *J. Mat. in Civ. Engrg.*, 22(7), 752–757.
- Van Wijk, K., Komatitsch, D., Scales, J. A., and Tromp, J. (2004). "Analysis of strong scattering at the micro-scale." *J Acoust Soc Am*, 115, 1006–1011.
- Voigt, T., Akkaya, Y., and Shah, S. P. (2003). "Determination of early age mortar and concrete strength by ultrasonic wave reflections." *J. Mat. in Civ. Engrg.*, 15(3), 247–254.

Queries

1. Please check that ASCE Membership Grades (Member ASCE, Fellow ASCE, etc.) are provided for all authors that are members. Also, please include the full location (eg., city, state, and/or country, as appropriate) for each author's affiliation.
2. under Experimental Process, 1st sentence, can you check: "water to cement ratio of 0.5 and sand to cement 2 by mass". Is something missing here? sand to cement ratio? Is 2 by mass correct?
3. Can you please check the caption in Fig. 2. Should this be as you set up Fig 6, for example: (a)....; (b)....(c)... Shouldn't the content come after (a), (b) and (c)?
4. A check of online databases revealed a possible error in this reference. (Aggelis, D. G., and Shiotani, T. [2007]) The page number has been changed from '151' to 'EL151'. Please confirm this is correct.
5. This query was generated by an automatic reference checking system. This reference (Aggelis, D. G., and Shiotani, T. [2008]) could not be located in the databases used by the system. While the reference may be correct, we ask that you check it so we can provide as many links to the referenced articles as possible.
6. For Kaplan, M.F. 1959, please provide links to this article as it could not be found by ASCE or me.
7. This query was generated by an automatic reference checking system. This reference (Kaplan, M. F. [1959]) could not be located in the databases used by the system. While the reference may be correct, we ask that you check it so we can provide as many links to the referenced articles as possible.